Commun Nonlinear Sci Numer Simulat 152 (2026) 109458

Contents lists available at ScienceDirect

Communications in Nonlinear Science and Numerical Simulation

journal homepage: www.elsevier.com/locate/cnsns

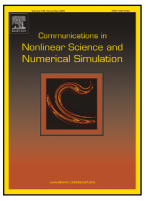

Research paper

Asynchronous observer-based control for input-to-state stability of Markov jump systems

Jian Liu [a], Luhao Jin [a], Lijuan Zha [b], Jinliang Liu [c,*], Yushun Tan [d]

[a] School of Computer and Artificial Intelligence, Nanjing University of Finance and Economics, NanJing, 210023, China
[b] School of Science, Nanjing Forestry University, Nanjing, 210037, China
[c] School of Computer Science, Nanjing University of Information Science and Technology, Nanjing, 210044, China
[d] School of Applied Mathematics, Nanjing University of Finance and Economics, Nanjing, 210023, China

ARTICLE INFO

Keywords:
Markov jump systems
Asynchronous control
Input-to-state stability
Adaptive dynamic event-triggered scheme
Encoding-decoding communication mechanism

ABSTRACT

This paper investigates the asynchronous control problem of Markov jump systems (MJSs) under an encoding-decoding communication mechanism. To alleviate the communication pressure on the channel caused by measurement signal filtering, zero-order hold (ZOH) technology and adaptive dynamic event-triggered scheme (ADETS) are employed. Furthermore, uniform quantization technology is integrated into the transmission channel between the sensors and the observer to achieve privacy protection, which further reduces the pressure of data transmission. Additionally, the paper addresses the issue of behavior mismatches between the controlled object and the controller modes that may arise due to denial of service attacks (DoSAs). It also considers the practical challenge where controllers often cannot fully obtain the mode information of the controlled system. To tackle this, a feedback controller based on asynchronous observers is designed, and a linearization method based on inequalities is employed to solve for the controller gain. The stability of the system under ADETSs, EDCM, and DoSAs is proven using sufficient conditions from input-to-state stability (ISS) theory and Lyapunov functions.

1. Introduction

In recent decades, networked control systems (NCSs) have experienced rapid development due to advancements in hardware technologies such as computers and sensors, as well as innovations in communication and control techniques. As a result, NCSs are now widely applied across various fields [1–8]. However, in practical applications, dynamic changes in control systems are inevitable due to environmental fluctuations, variations in component parameters, or alterations in system structure. Markov jump systems (MJSs) represent a type of dynamic system that includes a finite or infinite set of modes or subsystems. They effectively model random switching dynamics constrained by Markov chains, providing a robust mathematical framework for networked control systems. This framework facilitates a better understanding and optimization of their dynamic behavior and control strategies. Since the introduction of MJSs in the early 1960s, numerous scholars have made substantial contributions to the analysis of stability, controller synthesis, and filter design related to MJSs. Nowadays, MJSs have been widely used to model physical systems that experience structural and parameter random jumps, as well as sudden environmental disturbances. Examples include fault tolerant control systems [9], biological systems [10], and power grid systems [11–15].

As the potential of Markov jump systems (MJSs) continues to be explored across various fields, it has garnered increasing attention from researchers, becoming a focal point of study in recent decades. However, many existing studies rely on controllers that

* Corresponding author.
E-mail address: 003768@nuist.edu.cn (J. Liu).

https://doi.org/10.1016/j.cnsns.2025.109458
Received 17 March 2025; Received in revised form 21 June 2025; Accepted 27 October 2025
Available online 30 October 2025

operate synchronously with observers for MJSs. In practical scenarios, controllers often cannot fully obtain the mode information of the systems they control. Therefore, considering asynchronous control for MJSs is crucial. Zhang et al. [16] studied the security and asynchronous control problem of MJS in the context of non-periodic discrete DoSAs. Kuppusamy et al. [17] investigated the stabilization problem of discrete-time power systems affected by random jumps through asynchronous control. However, research on asynchronous control of MJSs remains limited. Therefore, designing asynchronous observers for MJSs continues to hold practical significance. In today's era of rapid development and widespread application of network technology, traditional systems are increasingly transitioning to networked control systems (NCSs). Wireless communication has gained popularity due to its flexibility, scalability, and low cost. However, the inherent vulnerabilities of open networks have made network security a pressing concern [18–20]. Among various security issues, scholars have made significant progress in studying the impact of DoSAs and developing strategies to mitigate the threats they pose [21–26]. Liu et al. [27] investigated the design problem of secure adaptive event-triggered filters under input constraints and mixed network attacks. A novel mixed network attack model was established, which considers various types of network attacks, including DoSAs, false data injection attacks (FDIAs) and replay attacks (RAs), for filter design. Zhao et al. [28] considered more realistic non-periodic DoSAs in the model and designed the attack frequency and duration based on real data. However, to our knowledge, there is limited research on the asynchronous stability control of MJSs under non-periodic DoSAs, which serves as one of the motivations for this paper. On the other hand, many practical applications face constrained network bandwidth, which has led to increased focus on efficient data transmission under such conditions. Event-triggered schemes (ETSs) are widely used to address issues related to network communication load and resource conservation. As a result, they have been extensively studied by numerous scholars [29–34]. Chen et al. [35] designed a novel dual-channel triggering control framework that enables semi-independent triggering for both input and output channels. Liu et al. [36] introduced a dynamic threshold scheme in the adaptive event-triggered scheme (ADETS) model to reduce network congestion. This approach considers bursty data to avoid unnecessary wastage of channel resources. Furthermore, the openness of network communications has introduced not only security and data transmission issues but also made privacy protection a focal point. In response, a unified quantization method for data encoding and decoding, known as the encoding-decoding communication mechanism (EDCM), has gained considerable attention [37–41]. EDCM enhances the utilization of network resources through efficient data processing and further reduces communication burdens, significantly improving data privacy and security. Gao et al. [42] proposed a novel EDCM for each sensor, consisting of two pairs of innovative encoders/decoders and estimation encoders/decoders. This scheme is designed to compress data to fit within bandwidth-constrained networks. However, EDCM is also susceptible to malicious attacks from the network, leading to performance degradation. Therefore, it is of paramount importance to consider the potential malicious attacks within the network while achieving efficient data transmission and privacy protection. This paper explores the input-state stability problem of MJS considering privacy protection and network attacks in asynchronous control. To ensure optimal performance of the MJS, a state feedback controller based on observers is designed. In order to tackle network communication issues, two independent ADETSs are implemented in the channels from the sensor to the observer (S/O) and from the controller to the actuator (C/A), respectively. The main contributions of this paper are as follows:

1. The system model discussed in this paper is comprehensive and addresses potential issues that may arise in practical applications. It considers behavior mismatches between the controlled object and the controller modes due to the effects of Denial of Service Attacks (DoSAs), as well as challenges such as limited bandwidth in specialized scenarios like underwater communication [43]. In contrast to the ideal environment examined in [39], this paper implements two independent Asynchronous Dynamic Event Triggering Systems (ADETS) in the Sensor/Observer (S/O) and Controller/Actuator (C/A) channels, respectively. Compared to traditional Event Triggering Systems (ETSs), the ADETSs utilized here demonstrate significantly higher efficiency in signal filtering.
2. A feedback controller based on an asynchronous observer has been designed to ensure that the MJS can achieve the desired performance. Additionally, the proposed controller and observer allow for independent switching modes, enabling the observer and controller to operate without the necessity of synchronizing with the controlled system, thus relaxing the operational requirements. Furthermore, a linearization method based on inequalities has been employed to determine the controller gains associated with the observer.
3. A reasonable EDCM has been adopted to achieve privacy protection, effectively preventing the theft and eavesdropping of user data. By leveraging the characteristics of EDCM alongside ADETS, the system can achieve improved data filtering, further alleviating network communication pressure. This approach ensures that the system maintains desired performance levels even under limited network bandwidth conditions.

The remaining arrangements of this article can be presented as follows. Section 2 outlines the depiction of MJS proposed in this article and provides a preliminary explanations. Section 3 elaborates on the results of the paper. Section 4 demonstrated a simulation example. Finally, Section 5 gives a conclusion.

2. Problem formulation

Fig. 1 illustrates the MJS under DoSAs, where measurement signals from the sensor to the observer are transmitted over the network using a designed EDCM. During this process, it is possible that the measurement signals may be subject to network attacks before reaching the observer.

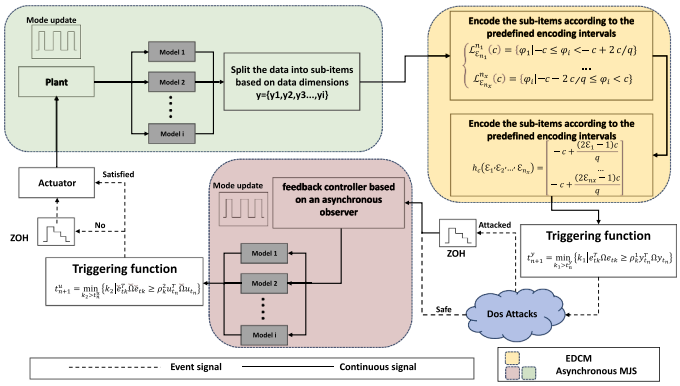

Fig. 1. The diagram of MJS under ADETSs, EDCM and DoSAs.

2.1. System model

In this paper, we focus on the category of discrete-time MJSs characterized by the following structure, inspired by [44]:

$$\begin{cases} x_{k+1} = A_{r_k} x_k + B_{r_k} u_k + D_{r_k} f(x_k) \\ y_k = C_{r_k} x_k \end{cases} \tag{1}$$

where $x_k \in \mathbb{R}^{n_x}$, $y_k \in \mathbb{R}^{n_y}$, $u_k \in \mathbb{R}^{n_u}$ represent the system state, the measurement signal and the control signal, respectively. The system state x_k possesses an initial state $x_0 = v_0$ such that $\|v_0\|_2 \le \epsilon_0$, where ϵ_0 being a known constant. A_{r_k}, B_{r_k}, D_{r_k} and C_{r_k} are constants determined by the Markov jump process. $f(\cdot)$ is a known nonlinear function satisfies $f(0) = 0$ and

$$\|f(z_k + \delta_k) - f(z_k)\|_2 \le \|G\delta_k\|_2 \tag{2}$$

where G is a known real matrix of the correct dimensions and $\delta_k \in \mathbb{R}^{n_x}$ is a vector. The subscript r_k represents a stochastic variable that is influenced by a Markov process, with its values confined to the set $\mathcal{L} = \{1, 2, 3, \dots, L\}$. The probabilities of transitions between different states of r_k are as follows:

$$Pr\{r_{k+1} = j | r_k = i\} = \pi_{ij} \tag{3}$$

where probabilities $\pi_{ij} \in [0,1]$ and $\sum_{i=1}^{L} \pi_{ij} = 1$ for $i, j \in \mathcal{L}$.

2.2. Observer design

The primary focus of this paper is to design a controller based on a dynamic observer that operates asynchronously with the controlled system. In practical scenarios, the observer/controller often cannot access the true system mode. Therefore, it is acceptable for the proposed observer-based controller to have entirely different switching modes from the system. This means that the observer-based control does not need to operate synchronously with the system, enhancing its practicality for real-world applications. Additionally, it is important to clarify that the asynchronicity mentioned here refers to mode asynchronicity, not time asynchronicity. The particular expressions of the observer and the controller are given as:

$$\begin{cases} \tilde{x}_{k+1} = A_{\tau_k} \tilde{x}_k + B_{\tau_k} u_k + D_{\tau_k} f(\tilde{x}_k) + L_{\tau_k}(y_k \\ \qquad\qquad - \tilde{y}_k) \\ \tilde{y}_k = C_{\tau_k} \tilde{x}_k \\ u_k = K_{\tau_k} \tilde{x}_k \\ \tilde{x}_0 = 0 \end{cases} \tag{4}$$

where $\tilde{x}_k \in \mathbb{R}^{n_x}$, $\tilde{y}_k \in \mathbb{R}^{n_y}$ are the observer state vector and the output variable of the observer estimation. The stochastic variable τ_k can be understood as a probabilistic mapping of r_k from the domain $\mathcal{L}$ to the set $\mathcal{S}$, where $\mathcal{S} = \{1, 2, 3, \dots, S\}$. The associated transition probability matrix $\theta = \{\theta_{iq}\}$ is defined as:

$$Pr\{\tau_k = q | r_k = i\} = \theta_{iq}, i \in \mathcal{L}, q \in \mathcal{S}, \tag{5}$$

where $0 \le \theta_{iq} \le 1$, $\sum_{q=1}^{S} \theta_{iq} = 1$ for all $i \in \mathcal{L}, q \in \mathcal{S}$. It is important to observe that the spaces $\mathcal{L}$ and $\mathcal{S}$ are independent. Specifically, $\mathcal{S}$ may either be larger than, smaller than, or equal to $\mathcal{L}$.

2.3. Adaptive event-triggered scheme

For control systems where the controller and sensor are not co-located, this paper proposes two independent ADETSs aimed at determining the appropriate timing for updating the sensor outputs and controller outputs. Two event generators are used to determine necessary sampled data to be transmitted. By denoting t_n^y as the last release instant of the first event generator, the next release instant of the first event generator can be determined by the following event-triggered condition:

$$t_{n+1}^y = \min_{k_1 > t_n^y} \{k_1 | e_{tk}^T \Omega e_{tk} \geq \rho_k^1 y_{t_n}^T \Omega y_{t_n}\} \tag{6}$$

where Ω is a positive matrix with appropriate dimensions; $e_{tk} = y_k - y_{t_n}$ represents the error in the measured output at the current sampling time, as well as at the preceding triggered time instant. $\rho_k^1 \in [\rho_m, \rho_M]$ is the adaptive threshold coefficient following the criterion $\rho_k^1 = \rho_M + (\rho_m - \rho_M)\frac{2}{\pi}\text{atan}\{\tau_1 \|y_k - y_{t_n}\|_2\}$, $\rho_0^1 = \rho_m$, for the given scalars $0 \leq \rho_m < \rho_M$; $\tau_1 > 0$ is used to adjust the sensitivity of ρ_k^1. The next release instant of the second event generator is the same:

$$t_{n+1}^u = \min_{k_2 > t_n^u} \{k_2 | \tilde{e}_{tk}^T \tilde{\Omega} \tilde{e}_{tk} \geq \rho_k^2 u_{t_n}^T \tilde{\Omega} u_{t_n}\} \tag{7}$$

where $\tilde{\Omega}$ is a positive matrix with appropriate dimensions; $\tilde{e}_{tk} = u_k - u_{t_n}$ represents the error in the control output at the current sampling time and at the previous triggered time instant. ρ_k^2 and τ_2 are the same as ρ_k^1 and τ_1. Denoting $e_k \triangleq x_k - \tilde{x}_k$ and $\tilde{f}(e_k) \triangleq f(x_k) - f(\tilde{x}_k)$, it can be inferred from (4) and (6) that:

$$\begin{aligned}
x_{k+1} &= A_{r_k} x_k + B_{r_k} u_{tn} + D_{r_k} f(x_k) \\
&= (A_{r_k} + B_{r_k} K_{\tau_k})\tilde{x}_k + A_{r_k} e_k - B_{r_k} \tilde{e}_{t_k} \\
&\quad + D_{r_k} f(x_k) \\
\tilde{x}_{k+1} &= A_{\tau_k} \tilde{x}_k + B_{\tau_k} u_{t_n} + D_{\tau_k} f(\tilde{x}_k) + L_{\tau_k}(y_k \\
&\quad - \tilde{y}_k) \\
&= (A_{\tau_k} + B_{\tau_k} K_{\tau_k})\tilde{x}_k - B_{\tau_k} \tilde{e}_{t_k} + D_{\tau_k} f(\tilde{x}_k) \\
&\quad + L_{\tau_k}(y_k - \tilde{y}_k) \\
e_{k+1} &= x_{k+1} - \tilde{x}_{k+1} \\
&= (A_{r_k} - A_{\tau_k} + B_{r_k} K_{r_k} - B_{\tau_k} K_{\tau_k})\tilde{x}_k + A_{r_k} e_k \\
&\quad + D_{r_k} f(x_k) - D_{\tau_k} f(\tilde{x}_k) - L_{\tau_k}(y_k - \tilde{y}_k).
\end{aligned} \tag{8}$$

To simplify the notation, we denote $r_k = i$ and $\tau_k = q$ respectively, then the closed-loop system can be expressed as

$$\begin{cases}
x_{k+1} = (A_i + B_i K_q)\tilde{x}_k + A_i e_k - B_i \tilde{e}_{t_k} + D_i f(x_k) \\
\tilde{x}_{k+1} = (A_q + B_q K_q)\tilde{x}_k - B_q \tilde{e}_{t_k} + D_q f(\tilde{x}_k) \\
\qquad\quad + L_q(y_k - \tilde{y}_k) \\
e_{k+1} = (A_i - A_q + B_i K_q - B_q K_q)\tilde{x}_k + A_i e_k \\
\qquad\quad - (B_i + B_q)\tilde{e}_{t_k} + D_i f(x_k) - D_q f(\tilde{x}_k) \\
\qquad\quad - L_q(y_k - \tilde{y}_k).
\end{cases} \tag{9}$$

Remark 1. For the design of the adaptive triggering threshold in (6), the trigonometric function $atan(\cdot)$ is employed. This function possesses the property of strict monotonicity across all intervals and satisfies the condition $0 \leq atan(x) \leq \frac{\pi}{2}$, $x \in [0, \infty)$. Leveraging this characteristic, in conjunction with parameters ρ_m, ρ_M and τ, facilitates the adaptive adjustment of the threshold derived from the error e_{t_k} and $\tilde{e}_{t_k}$.

Remark 2. According to the characteristics of the discrete nonlinear system as described by system Eq. (1), along with the definition of event triggering instants provided by (6) and (7), it can be observed that the lower bound of the interval between the current triggering moment t_k and the previous triggering moment t_{k-1} is 1. This indicates that the system triggers a finite number of times within any finite period, thereby avoiding the occurrence of Zeno behavior.

2.4. Uniform quantization technique and EDCM under DosAs

As a common signal processing technique, the uniform quantization technique is used to discretize continuous signals. Under this technique, the input signal is divided into uniformly sized intervals, and each interval is mapped to a discrete value. Below is a brief introduction to this technique: Given positive parameters κ and integer q, the hyperrectangle $\mathcal{F}_\kappa \triangleq \{\varphi \in \mathbb{R}^{n_x} : \|\varphi\|_2 \leq \kappa, i =$

$1,2,3,\dots,n_x\}$ can be divided into q^{n_x} hyperrectangles $\mathcal{L}^1_{\epsilon_1}(c)\times\mathcal{L}^2_{\epsilon_2}(c)\times\cdots\times\mathcal{L}^{n_x}_{\epsilon_{n_x}}(c)$, where $\epsilon_1,\epsilon_2,\dots,\epsilon_{n_x}\in\{1,2,\dots,q\}$ and

$$\begin{cases}\mathcal{L}^{n_1}_{\epsilon_{n_1}}(c)\triangleq\{\varphi_i|-c\le\varphi_i<-c+2c/q\}\\ \mathcal{L}^{n_2}_{\epsilon_{n_2}}(c)\triangleq\{\varphi_i|-c+2c/q\le\varphi_i<-c+4c/q\}\\ \quad\vdots\\ \mathcal{L}^{n_x}_{\epsilon_{n_x}}(c)\triangleq\{\varphi_i|c-2c/q\le\varphi_i<c\}\end{cases}\tag{10}$$

with φ_i being the ith element of the vector φ, The center of the hyperrectangle $\mathcal{F}_c\triangleq\{\varphi\in\mathbb{R}^{n_x}:\|\varphi\|_2\le c,i=1,2,3,\dots,n_x\}$ can be divided into q^{n_x} hyperrectangles $\mathcal{L}^1_{\epsilon_1}(c)\times\mathcal{L}^2_{\epsilon_2}(c)\times\cdots\times\mathcal{L}^{n_x}_{\epsilon_{n_x}}(c)$, where $\epsilon_1,\epsilon_2,\dots,\epsilon_{n_x}\in\{1,2,\dots,q\}$ is defined as

$$\hbar_c(\epsilon_1,\epsilon_2,\dots,\epsilon_{n_x})\triangleq\begin{bmatrix}-c+\frac{(2\epsilon_1-1)c}{q}\\ -c+\frac{(2\epsilon_2-1)c}{q}\\ \vdots\\ -c+\frac{(2\epsilon_{n_x}-1)c}{q}\end{bmatrix}.\tag{11}$$

Then, for any $\varphi\in\mathcal{F}_\kappa$, there exist unique integers $\epsilon_1,\epsilon_2,\dots,\epsilon_{n_x}\in\{1,2,\dots,q\}$, such that $\varphi\in\mathcal{L}^1_{\epsilon_1}(c)\times\mathcal{L}^2_{\epsilon_2}(c)\times\cdots\times\mathcal{L}^{n_x}_{\epsilon_{n_x}}(c)$, which indicates

$$\|\varphi-\hbar_c(\epsilon_1,\epsilon_2,\dots,\epsilon_{n_x})\|_2\le\frac{\sqrt{n_x}c}{q}.\tag{12}$$

The above is an introduction to the uniform quantization technique. Next, we describe the encoder and decoder under DoSAs. Let t_n be the encoding instant, and d_{t_n} be the decoding error, defined as $d_{t_n}=y_{t_n}-\check{y}_{t_n}$, where y_{t_n} is the measurement signal filtered after ADETS, and $\check{y}_{t_n}$ is the decoded state generated by the decoder. The specifics are described as follows: Encoder : For $\varphi\triangleq y_{t_n}\in\mathcal{L}^1_{\epsilon_1}(c)\times\mathcal{L}^2_{\epsilon_2}(c)\times\cdots\times\mathcal{L}^{n_x}_{\epsilon_{n_x}}(c)\subset\mathcal{F}_c(t_n)$, it follows

$$\begin{aligned}\theta_{t_n}&=\alpha_k[\epsilon_1,\epsilon_2,\dots,\epsilon_{n_x}]\\&=[\bar{\epsilon}_1,\bar{\epsilon}_2,\dots,\bar{\epsilon}_{n_x}]\end{aligned}\tag{13}$$

and then, the following expression can be obtained :

$$\bar{\hbar}\triangleq\begin{bmatrix}-c+\frac{(2\bar{\epsilon}_1-1)c}{q}\\ -c+\frac{(2\bar{\epsilon}_2-1)c}{q}\\ \vdots\\ -c+\frac{(2\bar{\epsilon}_{n_x}-1)c}{q}\end{bmatrix}\tag{14}$$

where α_k is a Bernoulli variable satisfying the following probabilities:

$$E\{\alpha_k=1\}=\bar{\alpha},E\{\alpha_k=0\}=1-\bar{\alpha}\tag{15}$$

where $\bar{\alpha}\in[0,1]$.

According to the decoded state $\check{y}_{tn}$ and DoSAs (13) , the decoder-based Observer (9) can be rewritten as

$$\begin{aligned}\tilde{x}_{k+1}&=(A_q+B_qK_q)\tilde{x}_k-B_q\tilde{e}_{t_k}+D_qf(\tilde{x}_k)\\&\quad+L_q(\alpha_k\check{y}_{t_n}-\tilde{y}_k)\\&=(A_q+B_qK_q)\tilde{x}_k-B_q\tilde{e}_{t_k}+D_qf(\tilde{x}_k)\\&\quad+L_q(\alpha_kC_i\tilde{x}_k+\alpha_ke_k-\alpha_ke_{t_k}-\alpha_kd_{t_n}\\&\quad-C_q\tilde{x}_k)\\&=(A_q+B_qK_q+\alpha_kL_qC_i-L_qC_q)\tilde{x}_k-B_q\tilde{e}_{t_k}\\&\quad+D_qf(\tilde{x}_k)+\alpha_kL_qC_ie_k-\alpha_kL_qe_{t_k}\\&\quad-\alpha_kL_qd_{t_n}\\&=(A_q+B_qK_q+\bar{\alpha}_kL_qC_i-L_qC_q)\tilde{x}_k-B_q\tilde{e}_{t_k}\\&\quad+D_qf(\tilde{x}_k)+\bar{\alpha}L_qC_ie_k-\bar{\alpha}_kL_qe_{t_k}-\bar{\alpha}_kL_qd_{t_n}\\&\quad+(\alpha_k-\bar{\alpha}_k)(L_qC_i\tilde{x}_k+L_qC_ie_k-L_qe_{t_k}\\&\quad-L_qd_{t_n})\end{aligned}\tag{16}$$

The error dynamics can also be rewritten as

$$\begin{aligned} e_{k+1} &= (A_i - A_q + B_iK_q - B_qK_q)\tilde{x}_k + A_ie_k \\ &\quad - (B_i + B_q)\tilde{e}_{t_k} + D_if(x_k) - D_qf(\tilde{x}_k) \\ &\quad - L_q(\alpha_kC_i\tilde{x}_k + \alpha_kC_ie_k - \alpha_ke_{t_k} - \alpha_kd_{t_n} \\ &\quad - C_q\tilde{x}_k) \\ &= (A_i - A_q + B_iK_q - B_qK_q + L_qC_q)\tilde{x}_k + \\ &\quad A_ie_k - (B_i + B_q)\tilde{e}_{t_k} + D_if(x_k) - D_qf(\tilde{x}_k) \\ &\quad - \alpha_kL_q(C_i\tilde{x}_k + C_ie_k - e_{t_k} - d_{t_n}) \end{aligned} \tag{17}$$

$$\begin{aligned} &= (A_i - A_q + B_iK_q - B_qK_q + L_qC_q \\ &\quad - \bar{\alpha}_kL_qC_i)\tilde{x}_k + A_ie_k - (B_i + B_q)\tilde{e}_{t_k} \\ &\quad - \bar{\alpha}_kL_qC_ie_k + D_if(x_k) - D_qf(\tilde{x}_k) \\ &\quad + \bar{\alpha}_kL_qe_{t_k} + \bar{\alpha}_kL_qd_{t_n} - (\alpha_k - \bar{\alpha}_k)L_q(C_i\tilde{x}_k \\ &\quad + C_ie_k - e_{t_k} - d_{t_n}) \end{aligned}$$

Remark 3. From the perspective of attackers, network attacks often have limited resources, thus their occurrences tend to be random and constrained. Therefore, It is reasonable to utilize a Bernoulli distribution to represent the randomness of attacks in (13).

Definition 1. [45]Consider the following system:

$$v_{k+1} = p(v_k, \bar{\omega}_k) \tag{18}$$

where v_k denotes the system state, $\bar{\omega}_k$ represents the exogenous signal. The above system is ISS if there exist a $\mathcal{KL}$ function $h(\cdot,\cdot)$ and a $\mathcal{K}$ class function $l(\cdot)$, such that

$$h(\|v_o\|_2, k) + l(\|\bar{\omega}_k\|_\infty) \geq \|v_k\|_2 \tag{19}$$

where $\|\bar{\omega}_k\|_\infty \triangleq \sup_k\{\|\bar{\omega}_k\|\}$.

Lemma 1. *[46].Given a matrix $B \in \mathbb{R}^{n_1\times n_2}$ with rank$(B) = n_1$, it can be expressed as $B = O[S\ 0]D^T$, where $O^TO = I$ and $DD^T = I$, derived from singular value decomposition. Let matrices $Y > 0$ with $Y_{11} \in \mathbb{R}^{n_1\times n_1}$ and $Y_{22} \in \mathbb{R}^{(n_2-n_1)\times(n_2-n_1)}$. There exists $\bar{Y}$ such that $BY = \bar{Y}B$ under the following condition:*

$$Y = D\begin{bmatrix} Y_{11} & * \\ 0 & Y_{22} \end{bmatrix}D^T. \tag{20}$$

Lemma 2. *[38]. Assume that there exist an ISS-Lyapunov function $V(\rho_t, t)$, a $\mathcal{I}$ class function $\vartheta(\cdot)$ and three $\mathcal{I}_\infty$ class functions $\chi_1(\cdot)$, $\chi_2(\cdot)$ and $\chi_3(\cdot)$, such that the following two inequalities:*

$$\chi_1(\|\rho_t\|_2) \leq V(t, \|\rho_t\|_2) \leq \chi_2(\|\rho_t\|_2) \tag{21}$$

and

$$V(\rho_{t+1}, t+1) - V(t, \rho_t) \leq -\chi_3(\|\rho_t\|_2) + \vartheta(\|v_t\|_2) \tag{22}$$

hold for all $\rho_t \in \mathbb{R}^n$ and $v_t \in \mathbb{R}^p$. Then, the nonlinear discretetime system is input-to-state stable. Furthermore, the functions $h(\cdot\ ,\ \cdot)$ and $l(\cdot)$ in Definition1 can be chosen as

$$h(\cdot\ ,\ t) = \chi_1^{-1}(\phi^k\chi_2(\cdot)),\quad 0 < \phi < 1 \tag{23}$$

and

$$l(\cdot) = \chi_1^{-1}(\chi_2(\chi_3^{-1}(\vartheta(\cdot)))),\quad 0 < \phi < 1 \tag{24}$$

where $\chi_1^{-1}(\cdot)$ stands for the inverse function of the monotone function $\chi_1(\cdot)$ and so does $\chi_3^{-1}(\cdot)$.

Remark 4. So far, the security control problem of nonlinear network systems under EDCM has been addressed. The main results include: (1) EDCM is used for data transmission in the sensor-to-observer channel, reducing the communication burden and enhancing resource utilization, while considering network attacks to improve data security; (2) Event-triggering mechanisms minimize unnecessary data transmission, decreasing the workload of system components during non-triggering periods.

3. Main results

In this section, we present several sufficient conditions using the Lyapunov function. These conditions establish that the closed-loop system described by Eq. (1) is Input-to-State Stable (ISS). The specifics are outlined as follows:

Theorem 1. *For given scalars $\rho_M \in [0,1)$ and $\bar{\alpha} \in (0,1)$, the closed-loop system under ADETS, DoSAs, EDCM can be guaranteed if there exist scalars L^1, L^2, $\mu_1 > 0$, $\mu_2 > 0$, gain matrices K_i, L_i and positive definite matrices M_{iq}, N_{iq}, P_i, Q_i such that*

$$\sum_{q=1}^{S} \theta_{iq} \begin{bmatrix} M_{iq} & * \\ 0 & N_{iq} \end{bmatrix} < \begin{bmatrix} P_i & * \\ 0 & Q_i \end{bmatrix} \tag{25}$$

$$\Xi \triangleq \begin{bmatrix} \Xi_{11} & * & * \\ \Xi_{21} & \Xi_{22} & * \\ \Xi_{31} & \Xi_{32} & \Xi_{33} \end{bmatrix} < 0 \tag{26}$$

where

$$\Xi_{11} = \begin{bmatrix} \hat{M}_{iq} & * & * & * \\ \rho_M C_i^T \Omega C_i & \hat{N}_{iq} & * & * \\ 0 & 0 & -I & * \\ 0 & 0 & 0 & -I \end{bmatrix},$$

$$\Xi_{21} = \begin{bmatrix} 0 & 0 & 0 & 0 \\ -\rho_M \Omega C_i & -\rho_M \Omega C_i & 0 & 0 \\ -\rho_M \tilde{\Omega} K_q & 0 & 0 & 0 \\ \rho_M K_q & 0 & 0 & 0 \end{bmatrix},$$

$$\Xi_{22} = \begin{bmatrix} -O & 0 & 0 & 0 \\ 0 & (\rho_M - 1)\Omega & 0 & 0 \\ 0 & 0 & (\rho_M - 1)\tilde{\Omega} & 0 \\ 0 & 0 & 0 & \tilde{\Omega}^{-1} \end{bmatrix},$$

$$\Xi_{31} = \begin{bmatrix} \bar{A}_{iq} & A_i - L^1 L_q C_i & D_q & 0 \\ L^2 L_q C_i & L^2 L_q C_i & 0 & 0 \\ \hat{A}_{iq} & A_i - L^1 L_q C_i & D_i - D_q & D_i \\ -L^2 L_q C_i & -L^2 L_q C_i & 0 & 0 \end{bmatrix},$$

$$\Xi_{32} = \begin{bmatrix} -L^1 L_q & -L^1 L_q & B_q & 0 \\ -L^2 L_q & -L^2 L_q & 0 & 0 \\ L^1 L_q & L^1 L_q & -B_i + B_q & 0 \\ L^2 L_q & L^2 L_q & 0 & 0 \end{bmatrix},$$

$$\Xi_{33} = \begin{bmatrix} -\check{P}_i^{-1} & * & * & * \\ 0 & -\check{P}_i^{-1} & * & * \\ 0 & 0 & -\check{Q}_i^{-1} & * \\ 0 & 0 & 0 & -\check{Q}_i^{-1} \end{bmatrix},$$

$$\hat{M}_{iq} = \rho_k C_i^T \Omega C_i - M_{iq} + U_1^T U_1$$
$$\hat{N}_{iq} = \rho_k C_i^T \Omega C_i - N_{iq} + U_2^T U_2$$
$$\bar{A}_{iq} = A_q + B_q K_q + \bar{\alpha} L_q C_i - L_q C_q$$
$$\hat{A}_{iq} = A_i + B_i K_q - A_q - B_q K_q - \bar{\alpha} L_q C_i + L_q C_q$$
$$L^1 \triangleq \bar{\alpha}, \quad L^2 \triangleq \sqrt{E\{(\alpha_k - \bar{\alpha})^2\}}$$

Proof. Construct the following Lyapunov function:

$$V(k) = \tilde{x}_k^T P_i \tilde{x}_k + e_k^T Q_i e_k \tag{27}$$

Define $V_1(k) = \tilde{x}_k^T P_i \tilde{x}_k$, $V_2(k) = e_k^T Q_i e_k$ and

$$\check{P}_i = \sum_{j=1}^{L} \pi_{ij} P_j, \quad \check{Q}_i = \sum_{j=1}^{L} \pi_{ij} Q_j, \tag{28}$$

then calculate the difference of (26) along the trajectories of (16), (17) and take the corresponding expectation. It yields

$$\begin{aligned}
&E\{\Delta V_1(k)\}\\
&=\sum_{q=1}^{S}\theta_{iq}\tilde{x}_{k+1}^T\breve{P}_i\tilde{x}_{k+1}-\tilde{x}_k^T P_i\tilde{x}_k\\
&=\xi^T(k)(\sum_{q=1}^{S}\theta_{iq}\mathcal{X}_{iq}^T\breve{P}_i\mathcal{X}_{iq})\xi(k)-\tilde{x}_k^T P_i\tilde{x}_k\\
&\quad+\sum_{q=1}^{S}\theta_{iq}\sqrt{E\{(\alpha_k-\bar{\alpha})^2\}}(L_qC_i\tilde{x}_k+L_qC_ie_k\\
&\quad-L_qe_{t_k}-L_qd_{t_n})^T\breve{P}_i(L_qC_i\tilde{x}_k+L_qC_ie_k-L_qe_{t_k}\\
&\quad-L_qd_{t_n}),
\end{aligned}\tag{29}$$

where $\mathcal{X}_{iq}=[\hat{A}_{iq}\ \ \bar{\alpha}_kL_qC_i\ \ D_q\ \ 0\ \ -\bar{\alpha}_kL_q\ \ -\bar{\alpha}_kL_q\ \ -B_q]$ and $\xi(k)=[\tilde{x}_k^T\ \ e_k^T\ \ f^T(\tilde{x}_k)\ \ f^T(e_k)\ \ d_{t_n}^T\ \ e_{tk}^T\ \ \tilde{e}_{tk}^T]$. Likewise, it can be confirmed that

$$\begin{aligned}
&E\{\Delta V_2(k)\}\\
&=\sum_{q=1}^{S}\theta_{iq}\tilde{e}_{k+1}^T\breve{Q}_i\tilde{e}_{k+1}-e_k^TQ_ie_k\\
&=\xi^T(k)(\sum_{q=1}^{S}\theta_{iq}\mathcal{V}_{iq}^T\breve{P}_i\mathcal{V}_{iq})\xi(k)-e_k^TP_ie_k\\
&\quad+\sum_{q=1}^{S}\theta_{iq}\sqrt{E\{(\alpha_k-\bar{\alpha})^2\}}(L_qC_i\tilde{x}_k+L_qC_ie_k\\
&\quad-L_qe_{tk}-L_qd_{t_n})^T\breve{Q}_i(L_qC_i\tilde{x}_k+L_qC_ie_k-L_qe_{tk}\\
&\quad-L_qd_{t_n}),
\end{aligned}\tag{30}$$

where $\mathcal{V}_{iq}=[\hat{C}_{iq}A_i-\bar{\alpha}_kL_qC_iD_i-D_qD_i\bar{\alpha}_kL_q\bar{\alpha}_kL_q-B_q-B_i]$. Because of the condition (25), we can conclude that

$$\sum_{q=1}^{S}\theta_{iq}(diag\{M_{iq},\ N_{iq}\})\le\mathrm{diag}\{P_i,Q_i\}\tag{31}$$

Then, it can be obtained that

$$\begin{aligned}
&E\{\Delta V(k)\}\\
&=\xi^T(k)(\sum_{q=1}^{S}\theta_{iq}\mathcal{G}_{iq}\mathrm{diag}\{\breve{P}_i,\breve{Q}_i\}\mathcal{G}_{iq})\xi(k)\\
&\quad-\eta^T(k)(\mathrm{diag}\{P_i,Q_i\})\eta(k)\\
&\le\xi^T(k)(\sum_{q=1}^{S}\theta_{iq}\mathcal{G}_{iq}\mathrm{diag}\{\breve{P}_i,\breve{Q}_i\}\mathcal{G}_{iq})\xi(k)\\
&\quad-\eta^T(k)(\mathrm{diag}\{M_{iq},N_{iq}\})\eta(k)+\rho_k^1u_{t_n}^T\tilde{\Omega}u_{t_n}\\
&\quad-\tilde{e}_{tk}^T\tilde{\Omega}\tilde{e}_{tk}+\rho_k^2y_{t_n}^T\Omega y_{t_n}-e_{tk}^T\Omega e_{tk}+d_{t_n}^TOd_{t_n}\\
&\quad-d_{t_n}^TOd_{t_n}+\mu_1\tilde{x}_k^TU_1^TU_1\tilde{x}_k-\mu_1f^T(\tilde{x}_k)f(\tilde{x}_k)\\
&\quad+\mu_2e_k^TU_2^TU_2e_k-\mu_2f^T(e_k)f(e_k)\\
&=\xi^T(k)\Xi\xi(k)+d_{t_n}^TOd_{t_n}
\end{aligned}\tag{32}$$

According to (26), which implies that $\Xi<0$. Denoting $\zeta_k^T=\begin{bmatrix}\tilde{x}_k^T & e_k^T\end{bmatrix}$, $P=\begin{bmatrix}P_i & 0\\ 0 & Q_i\end{bmatrix}$, so $\|\zeta_0\|_2\le\sqrt{2}\epsilon_0$, it can be obtained that $\Delta V_k\le-\lambda_{min}(-\Xi)\|\zeta_k\|_2^2+\lambda_{max}\|d_{t_n}\|_2^2$. The System (1) is input-to-state stable by choosing

$$\begin{aligned}
&\vartheta(\|d_{t_n}\|_2)=\lambda_{max}(O)\|d_{t_n}\|_2^2,\\
&\chi_1(\|\zeta_k\|_2)=\lambda_{min}(P)\|\zeta_k\|_2^2,\\
&\chi_2(\|\zeta_k\|_2)=\lambda_{max}(P)\|\zeta_k\|_2^2,\\
&\chi_3(\|\zeta_k\|_2)=\lambda_{min}(-\Xi)\|\zeta_k\|_2^2,
\end{aligned}$$

then, letting

$$h(\|\zeta_0\|_2, k) = \sqrt{\frac{\phi^k \lambda_{max}(P)\|\sqrt{2}\epsilon_0\|_2^2}{\lambda_{min}(P)}},$$
$$l(\|d_{t_n}\|_2) = \sqrt{\frac{\lambda_{max}(P)\lambda_{max}(O)\|d_{t_n}\|_2^2}{\gamma\lambda_{min}(P)\lambda_{min}(-\xi)}} \tag{33}$$

with $0 < \gamma < 1$, we have from Definition 2 that

$$\|\zeta_k\|_2 \le h(\|\zeta_0\|_2, k) + l(\|d_{t_n}\|_2) \tag{34}$$

which completes the proof. □

3.1. Inequalities based linearization

In this section, we adopt an inequality-based linearization method from reference [47]. Before presenting the linearization results, we assume that the output matrix C_i is constant and has full row rank, meaning $C_i = C$.Under this assumption, it is feasible to perform singular value decomposition (SVD) on matrix C. More specifically, we decompose C as follows:

$$C = V_1[V_2 \quad 0]V_3^T \tag{35}$$

with

$$V_1V_1^T = I, \ \ V_3V_3^T = I, \tag{36}$$

which helps streamline the subsequent design processes.

Theorem 2. *For given scalars ρ_M and $\bar{\alpha}$, the closed-loop system can be guaranteed if there exist scalars L^1, L^2, $\mu_1 > 0$, $\mu_2 > 0$, and positive definite matrices $\bar{P}_i$, $\bar{Q}_i$, $\check{M}_{i,q}$, $\check{N}_{i,q}$, Z_1, Z_2, Z_3, $\bar{K}_q$ and $\bar{L}_q$ such that*

$$\sum_{q=1}^{S}\theta_{iq}\begin{bmatrix}\check{M}_{iq} & * \\ 0 & \check{N}_{iq}\end{bmatrix} < \begin{bmatrix}\bar{P}_i & * \\ 0 & \bar{Q}_i\end{bmatrix} \tag{37}$$

$$\bar{\Xi} \triangleq \begin{bmatrix}\bar{\Xi}_{11} & * & * \\ \bar{\Xi}_{21} & \bar{\Xi}_{22} & * \\ \bar{\Xi}_{31} & \bar{\Xi}_{32} & \bar{\Xi}_{33}\end{bmatrix} < 0 \tag{38}$$

where

$$\bar{\Xi}_{11} = \begin{bmatrix}\check{M}_{iq} & * & * & * \\ \rho_M C^T\Omega CZ & \check{N}_{iq} & * & * \\ 0 & 0 & -I & * \\ 0 & 0 & 0 & -I\end{bmatrix}, \bar{\Xi}_{21} = \begin{bmatrix}0 & 0 & 0 & 0 \\ -\rho_M\Omega CZ & -\rho_M\Omega CZ & 0 & 0 \\ -\rho_M\tilde{\Omega}\bar{K}_q & 0 & 0 & 0 \\ \rho_M\bar{K}_q & 0 & 0 & 0\end{bmatrix},$$
$$\bar{\Xi}_{22} = \begin{bmatrix}-O & 0 & 0 & 0 \\ 0 & (\rho_M - 1)\Omega & 0 & 0 \\ 0 & 0 & (\rho_M - 1)\tilde{\Omega} & 0 \\ 0 & 0 & 0 & \tilde{\Omega}^{-1}\end{bmatrix},$$
$$\bar{\Xi}_{31} = \begin{bmatrix}\check{A}_{iq} & A_iZ - L^1\bar{L}_qEV_3^T & D_q & 0 \\ L^2\check{L}_qEV_3^T & L^2\bar{L}_qEV_3^T & 0 & 0 \\ \check{A}_{iq} & A_iZ - L^1\bar{L}_qEV_3^T & D_i - D_q & D_i \\ -L^2L_qCZ & -L^2\bar{L}_qEV_3^T & 0 & 0\end{bmatrix},$$
$$\bar{\Xi}_{32} = \begin{bmatrix}-L^1L_q & -L^1L_q & B_q & 0 \\ -L^2L_q & -L^2L_q & 0 & 0 \\ L^1L_q & L^1L_q & -B_i + B_q & 0 \\ L^2L_q & L^2L_q & 0 & 0\end{bmatrix},$$
$$\bar{\Xi}_{33} = \begin{bmatrix}\Psi_1 & * & * & * \\ 0 & \Psi_1 & * & * \\ 0 & 0 & \Psi_2 & * \\ 0 & 0 & 0 & \Psi_2\end{bmatrix},$$

where

$$\begin{aligned}
&\check{M}_{iq} = Z^T\rho_k C^T\Omega C Z - Z^T M_{iq} Z + Z^T U_1^T U_1 Z,\\
&\check{N}_{iq} = Z^T\rho_k C^T\Omega C Z - Z^T N_{iq} Z + Z^T U_2^T U_2 Z,\\
&\check{A}_{iq} = A_q Z + B_q\bar{K}_q + L^1\bar{L}_q E V_3^T - \bar{L}_q E V_3^T\\
&\tilde{A}_{iq} = A_i Z + B_i\bar{K}_q - A_q Z - B_q\bar{K}_q - L^1\bar{L}_q E V_3^T + \bar{L}_q E V_3^T\\
&E = [I\ \ 0],\quad Z = V_3\begin{bmatrix} V_2^{-1}V_1^T Z_1 & 0\\ Z_2 & Z_3\end{bmatrix}V_3^T\\
&\Psi_1 = \sum_{j=1}^{L}\pi_{ij}\bar{P}_j - Z - Z^T,\ \Psi_2 = \sum_{j=1}^{L}\pi_{ij}\bar{Q}_j - Z - Z^T.
\end{aligned}$$

Then, the gains for the controller and observer can be expressed as:

$$K_q = \bar{K}_q Z^{-1},\quad L_q = \bar{L}_q Z^{-1}. \tag{39}$$

Proof. For ease of later linearization manipulations, matrices $\bar{P}_i$, $\bar{Q}_i$, $\check{M}_{i,q}$, $\check{N}_{i,q}$ have been defined as

$$\begin{aligned}
&\bar{P}_i = Z^T P_i Z,\quad \bar{Q}_i = Z^T Q_i Z\\
&\check{M} = Z^T M_{i,q} Z,\quad \check{N} = Z^T N_{i,q} Z.
\end{aligned} \tag{40}$$

It is apparent that by pre-multiplying and post-multiplying diag $\{(Z^T)^{-1}, (Z^T)^{-1}\}$ and its transpose, the inequality (37) holds true under condition (25). Importantly, we have $\check{P}_i = \sum_{j=1}^{L}\pi_{ij}P_j$ and $\check{Q}_i = \sum_{j=1}^{L}\pi_{ij}Q_j$ as stated in Theorem 1. Therefore, we arrive at the conclusion that

$$\begin{aligned}
&Z^T(\sum_{j=1}^{L}\pi_{ij}Q_j)Z - Z - Z^T > -(\sum_{j=1}^{L}\pi_{ij}Q_j)^{-1},\\
&Z^T(\sum_{j=1}^{L}\pi_{ij}P_j)Z - Z - Z^T > -(\sum_{j=1}^{L}\pi_{ij}P_j)^{-1},
\end{aligned} \tag{41}$$

which are equivalent to

$$\begin{aligned}
&(\sum_{j=1}^{L}\pi_{ij}\bar{Q}_j) - Z - Z^T > -(\check{P}_i)^{-1},\\
&(\sum_{j=1}^{L}\pi_{ij}\bar{P}_j) - Z - Z^T > -(\check{Q}_i)^{-1}.
\end{aligned} \tag{42}$$

Next, by integrating condition (38) with inequalities (42), it becomes clear that

$$\tilde{\Xi} \triangleq \begin{bmatrix} \bar{\Xi}_{11} & * & *\\ \bar{\Xi}_{21} & \bar{\Xi}_{22} & *\\ \bar{\Xi}_{31} & \bar{\Xi}_{32} & \Xi_{33}\end{bmatrix} < 0 \tag{43}$$

Then, the poof is finished. □

4. Simulation example

In this section, the rationality and feasibility of the proposed MJS under EDCM, ADETSs, and DoSAs are primarily demonstrated through numerical examples. In addition, the effectiveness of the proposed EDCM approach is further verified through experiments on an independent dataset and a series of image processing tasks. Consider the MJS (1) with parameters

$$\begin{aligned}
&A_1 = \begin{bmatrix}0.6 & 0.38\\ 0.32 & 0.50\end{bmatrix}, B_1 = \begin{bmatrix}-0.45\\ -0.35\end{bmatrix}, D_1 = \begin{bmatrix}0.24 & -0.6\\ 0.2 & 0.4\end{bmatrix},\\
&A_2 = \begin{bmatrix}0.30 & 0.50\\ 0.60 & 0.30\end{bmatrix}, B_2 = \begin{bmatrix}-0.25\\ -0.45\end{bmatrix}, D_2 = \begin{bmatrix}0.40 & -0.55\\ 0.30 & 0.60\end{bmatrix},\\
&C = C_1 = C_2 = \begin{bmatrix}0.8 & 0.8\end{bmatrix},\ U_1 = U_2 = \begin{bmatrix}0.1 & 0\\ 0 & 0.1\end{bmatrix}.
\end{aligned}$$

and the nonlinear function is selected as

$$f(x_k) = \begin{bmatrix}0.1x_{1,k} - tanh(0.05x_{1,k})\\ 0.2x_{2,k}\end{bmatrix}.$$

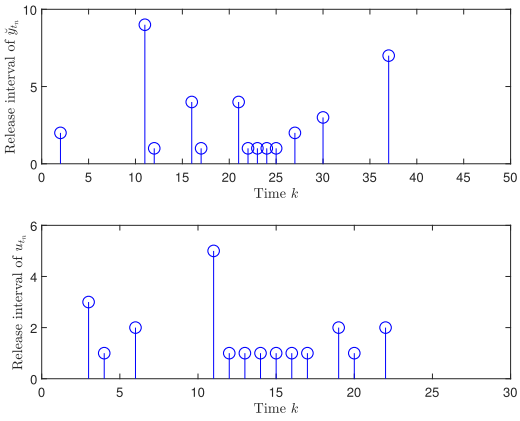

Fig. 2. Release instants of y_k and u_k under ADETSs.

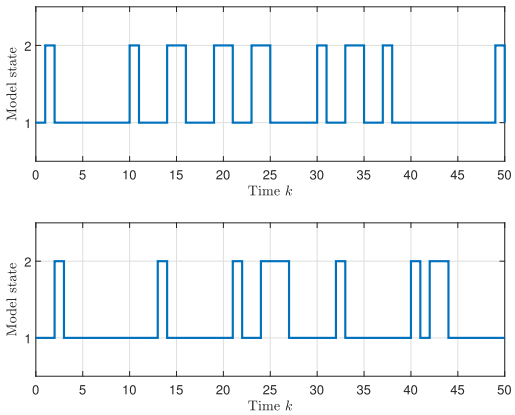

Fig. 3. Asynchronous switching of system modes in MJS.

The transition matrices of system (3) and observer-based controller (5) are provided as follows

$$\pi_{ij} = \begin{bmatrix} 0.8 & 0.2 \\ 0.9 & 0.1 \end{bmatrix}, \theta_{ij} = \begin{bmatrix} 0.7 & 0.3 \\ 0.6 & 0.4 \end{bmatrix}.$$

Meanwhile, the other parameters for EDCM, DoSAs and ADETSs are chosen as $c = 0.1$, $q = 1000$, $\bar{\alpha} = 0.8$, $\rho_M = 0.15$, $\rho_m = 0.1$, $\tau_1 = \tau_2 = 15$ and $\Omega = 1$. Furthermore, L^1 and L^2 can be caculated as 0.8 and 0.4.

Additionally, the gains of asynchronous observer and feedback controller can be obtained:

$$K_1 = \begin{bmatrix} 0.1164 & -0.1802 \end{bmatrix}, L_1 = \begin{bmatrix} 0.3381 \\ 0.7992 \end{bmatrix}$$

$$K_2 = \begin{bmatrix} 0.4482 & 0.5223 \end{bmatrix}, L_2 = \begin{bmatrix} 0.5484 \\ -0.1480 \end{bmatrix}.$$

In what follows, Fig. 2 presents the signal triggering frequency of the ADETSs deployed in the S/O and C/A channels. It is clearly demonstrated that the ADETSs significantly reduce the frequency of signal releases and can be adjusted according to signal variations. Therefore, the employment of ADETSs in this paper is more reasonable compared to traditional AETS.

Moreover, Fig. 3 illustrates the mode-switching behavior of the system described by Eq. (1) and the controller represented by Eq. (4), both of which are based on asynchronous observers. It is clear that the operations of these two entities occur asynchronously. Additionally, the system (1) is evidently unstable under the specified parameters. Figs. 4 and 5 present the corresponding state trajectories of the system when utilizing the state feedback controller based on asynchronous observers, as well as the discrepancies between the two. This effectively demonstrates that the asynchronous observer and controller designed in this paper are capable of accurately estimating the system state and enabling the system to achieve the desired performance. Furthermore, Fig. 6 displays the trajectory of the control input for the state feedback controller based on the asynchronous observer, providing additional insights into the controller's performance.

To demonstrate the effectiveness of the EDCM adopted in this paper, Fig. 7 records the performance of this EDCM in the test data. It can be clearly observed that throughout the process, the original signal closely overlaps with the signal processed by EDCM,

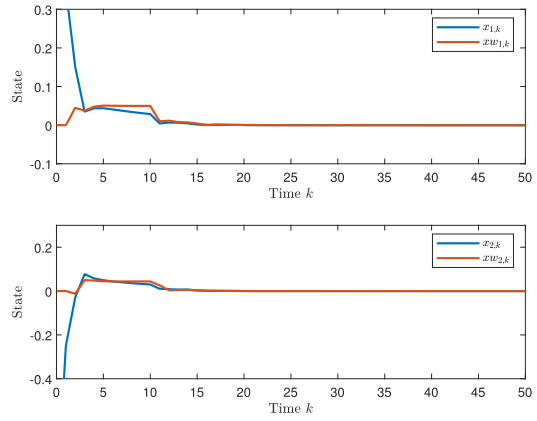

Fig. 4. System state x and corresponding state estimation $\hat{x}$.

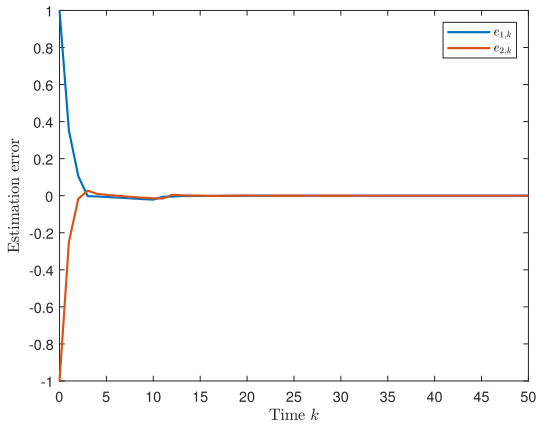

Fig. 5. Estimation error of system state $e_{1,k}$ and $e_{2,k}$.

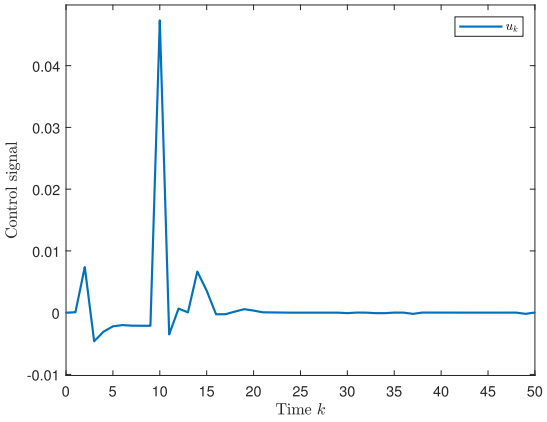

Fig. 6. Control Signals u_k.

resulting in a small overall error, thus confirming the validity of the EDCM. Subsequently, as shown in the Fig. 8, the employed EDCM maintains good performance under both ADETS and DoSAs. It is clear that, influenced by ADETS and DoSAs, the encoding and decoding errors are relatively larger; however, they still remain within a small range. Furthermore, as the system stabilizes, the error between the decoded signal and the original signal gradually converges to zero in both cases, thereby further validating the effectiveness of EDCM.

In addition, we conducted experiments to assess its feasibility for image encryption. Fig.9 illustrates the original image along with the scatter plot of the corresponding RGB color value distributions, while Figs.10 and 11 present the histograms of RGB color values

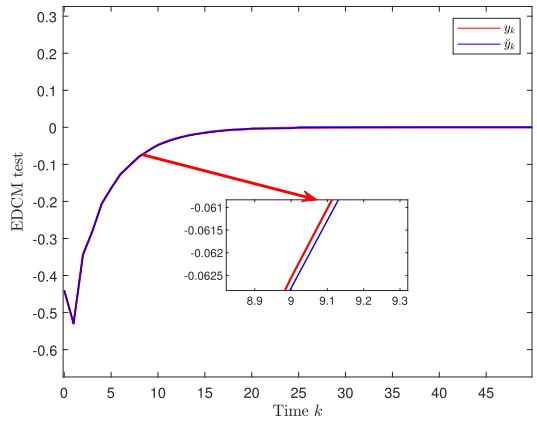

Fig. 7. EDCM under ideal conditions(without ADETS).

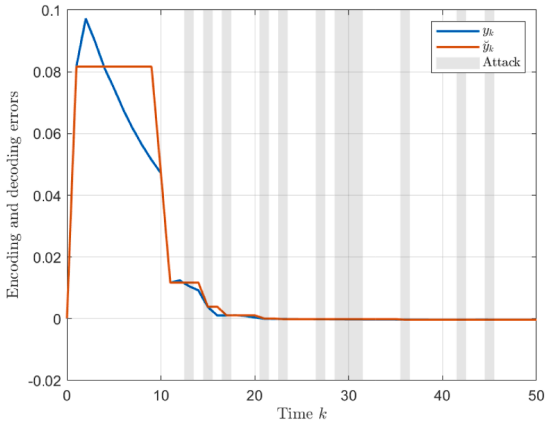

Fig. 8. EDCM under ADTES and DoSAs.

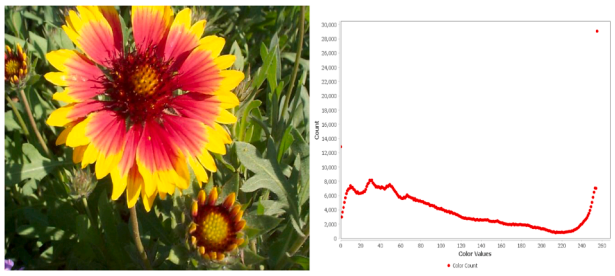

Fig. 9. Original image and color value distribution.

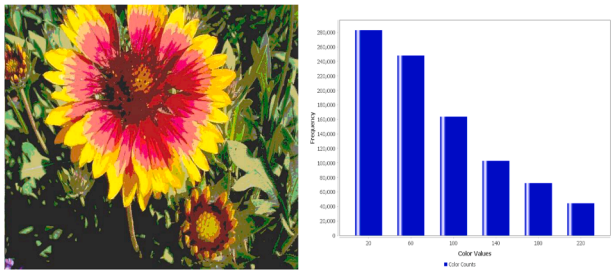

Fig. 10. EDCM-processed image and color values distribution ($q = 50$).

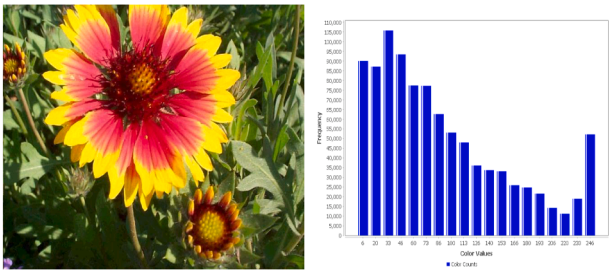

Fig. 11. EDCM-processed image and color values distribution ($q = 200$).

after EDCM processing with different parameters. It is clear from these figures that the distribution of RGB color values is significantly streamlined following EDCM, with the accuracy of color value categorization depending on the parameter q.

The streamlined data also suggests that the EDCM method can somewhat alleviate the demands of network communication. Figs.10 and 11 display the original image processed with EDCM using two different parameters, q = 50 and q = 200. It is evident that the implementation of EDCM not only aids in privacy protection but also effectively retains the original information of the image.

5. Conclusion

This paper investigates the MJSs control problem based on asynchronous observers under DoSAs conditions. It considers the possibility of a mismatch between the dynamics of the controlled object and the controller modes due to the influence of DoSAs. Furthermore, to alleviate bandwidth pressure during signal transmission and conserve channel resources, two independent ADETSs are employed in the S/O and C/A channels to prevent data congestion. In addition, the ZOH technique is utilized to transmit data at non-triggered times, ensuring the normal operation of the system during these intervals. Uniform quantization is also applied to compress data through EDCM, further reducing channel resource consumption and enhancing data transmission security. Moreover, a linearization approach based on inequalities is employed to derive the controller gain based on asynchronous observers. Conditions for ensuring the ISS of the closed-loop system are established using Lyapunov function, and the feasibility of this method is validated through a numerical example.

CRediT authorship contribution statement

Jian Liu: Writing – review & editing, Methodology, Investigation; **Luhao Jin:** Writing – original draft, Software; **Lijuan Zha:** Visualization, Formal analysis; **Jinliang Liu:** Project administration, Conceptualization; **Yushun Tan:** Supervision, Resources.

Data availability

No data was used for the research described in the article.

Declaration of competing interests

The authors declare that they have no known competing financial interests or personal relationships that could have appeared to influence the work reported in this paper.

Acknowledgment

This work was supported in part by the National Natural Science Foundation of China under Grant 62001210, Grant 62441310, and Grant 62373252, in part by the Young Elite Scientists Sponsorship Program by JSAST under Grant JSTJ-2025-452, in part by the Startup Foundation for Introducing Talent of NUIST under Grant 2024r063.

References

[1] Wang T, Gao H, Qiu J. A combined adaptive neural network and nonlinear model predictive control for multirate networked industrial process control. IEEE Trans Neural Netw Learn Syst 2016;27(2):416–25. https://doi.org/10.1109/TNNLS.2015.2411671

[2] Yang J, Liu CC, Tse CK, Huang M. Stability analysis and design of islanded microgrids integrating pinning-based and consensus-based distributed secondary control. IEEE Trans Power Electron 2024. https://doi.org/10.1109/TPEL.2024.3402440

[3] Yogi SC, Behera L, Tripathy T. Neural-fxSMC: A robust adaptive neural fixed-time sliding mode control for quadrotors with unknown uncertainties. IEEE Rob Autom Lett 2024;9(6):5927–34. https://doi.org/10.1109/LRA.2024.3398425

[4] Heshmati-Alamdari S, Karras GC, Marantos P, Kyriakopoulos KJ. A robust predictive control approach for underwater robotic vehicles. IEEE Tran Control Syst Technol 2020;28(6):2352–63. https://doi.org/10.1109/TCST.2019.2939248

[5] Klügel M, Mamduhi M, Ayan O, Vilgelm M, Johansson KH, Hirche S, et al. Joint cross-layer optimization in real-time networked control systems. IEEE Trans Control Netw Syst 2020;7(4):1903–15. https://doi.org/10.1109/TCNS.2020.3011847

[6] Nilsson G, Como G. Generalized proportional allocation policies for robust control of dynamical flow networks. IEEE Trans Autom Control 2022;67(1):32–47. https://doi.org/10.1109/TAC.2020.3046026

[7] Ganapathy K, Ruths J, Summers T. Performance bounds for optimal and robust feedback control in networks. IEEE Trans Control Netw Syst 2021;8(4):1754–66. https://doi.org/10.1109/TCNS.2021.3084453

[8] Shah D, Mehta A, Patel K, Bartoszewicz A. Event-triggered discrete higher-order SMC for networked control system having network irregularities. IEEE Trans Ind Inf 2020;16(11):6837–47. https://doi.org/10.1109/TII.2020.2973739

[9] Dong S, Liu M, Wu Z-G, Shi K. Observer-based sliding mode control for markov jump systems with actuator failures and asynchronous modes. IEEE Trans Circuits Syst II Express Briefs 2021;68(6):1967–71. https://doi.org/10.1109/TCSII.2020.3030703

[10] Meng M, Liu L, Feng G. Stability and l_1 gain analysis of Boolean networks with Markovian jump parameters. IEEE Trans Autom Control 2017;62(8):4222–8. https://doi.org/10.1109/TAC.2017.2679903

[11] Lai J, Lu X, Monti A, Liu G-P. Stochastic distributed pinning control for co-multi-inverter networks with a virtual leader. IEEE Trans Circuits Syst II Express Briefs 2020;67(10):2094–8. https://doi.org/10.1109/TCSII.2019.2950764

[12] Dong S, Liu M. Adaptive fuzzy asynchronous control for nonhomogeneous Markov jump power systems under hybrid attacks. IEEE Trans Fuzzy Syst 2023;31(3):1009–19. https://doi.org/10.1109/TFUZZ.2022.3193805

[13] Das P, Shuvro RA, Povinelli K, Sorrentino F, Hayat MM. Mitigating cascading failures in power grids via markov decision-based load-shedding with DC power flow model. IEEE Syst J 2022;16(3):4048–59. https://doi.org/10.1109/JSYST.2022.3175359

[14] Roça IL, Carvalho P MS. Solving ill-conditioned state-estimation problems in distribution grids with hidden-Markov models of load dynamics. IEEE Trans Power Syst 2020;35(1):284–92. https://doi.org/10.1109/TPWRS.2019.2928211

[15] Marzband M, Azarinejadian F, Savaghebi M, Guerrero JM. An optimal energy management system for islanded microgrids based on multiperiod artificial bee colony combined with Markov chain. IEEE Syst J 2017;11(3):1712–22. https://doi.org/10.1109/JSYST.2015.2422253

[16] Zhang Y, Wu Z-G. Asynchronous control of Markov jump systems under aperiodic dos attacks. IEEE Trans Circuits Syst II Express Briefs 2023;70(2):685–9. https://doi.org/10.1109/TCSII.2022.3211930

[17] Kuppusamy S, Joo YH, Kim HS. Asynchronous control for discrete-time hidden Markov jump power systems. IEEE Trans Cybern 2022;52(9):9943–8. https://doi.org/10.1109/TCYB.2021.3062672

[18] Esmalifalak M, Liu L, Nguyen N, Zheng R, Han Z. Detecting stealthy false data injection using machine learning in smart grid. IEEE Syst J 2017;11(3):1644–52. https://doi.org/10.1109/JSYST.2014.2341597

[19] Drayer E, Routtenberg T. Detection of false data injection attacks in smart grids based on graph signal processing. IEEE Syst J 2020;14(2):1886–96. https://doi.org/10.1109/JSYST.2019.2927469

[20] Boyaci O, Umunnakwe A, Sahu A, Narimani MR, Ismail M, Davis KR, et al. Graph neural networks based detection of stealth false data injection attacks in smart grids. IEEE Syst J 2022;16(2):2946–57. https://doi.org/10.1109/JSYST.2021.3109082

[21] He W, Xu W, Ge X, Han Q-L, Du W, Qian F. Secure control of multiagent systems against malicious attacks: A brief survey. IEEE Trans Ind Inf 2022;18(6):3595–608. https://doi.org/10.1109/TII.2021.3126644

[22] Qi W, Lv C, Zong G, Ahn CK. Sliding mode control for fuzzy networked semi-Markov switching models under cyber attacks. IEEE Trans Circuits Syst II Express Briefs 2022;69(12):5034–8. https://doi.org/10.1109/TCSII.2021.3137196

[23] Deng C, Wen C. Mas-based distributed resilient control for a class of cyber-physical systems with communication delays under dos attacks. IEEE Trans Cybern 2021;51(5):2347–58. https://doi.org/10.1109/TCYB.2020.2972686

[24] De Miranda RV, Inácio P RM, Magoni D, Freire MM. Detection and mitigation of low-rate denial-of-service attacks: A survey. IEEE Access 2022;10:76648–68. https://doi.org/10.1109/ACCESS.2022.3191430

[25] Doostmohammadian M, Meskin N. Finite-time stability under denial of service. IEEE Syst J 2021;15(1):1048–55. https://doi.org/10.1109/JSYST.2020.2992702

[26] Li S, Ahn CK, Xiang Z. Decentralized sampled-data control for cyber-physical systems subject to dos attacks. IEEE Syst J 2021;15(4):5126–34. https://doi.org/10.1109/JSYST.2020.3019939

[27] Liu J, Wang Y, Cao J, Yue D, Xie X. Secure adaptive-event-triggered filter design with input constraint and hybrid cyber attack. IEEE Trans Cybern 2021;51(8):4000–10. https://doi.org/10.1109/TCYB.2020.3003752

[28] Zhao N, Shi P, Xing W, Agarwal RK. Resilient event-triggered control for networked cascade control systems under denial-of-service attacks and actuator saturation. IEEE Syst J 2022;16(1):1114–22. https://doi.org/10.1109/JSYST.2021.3066540

[29] Yue D, Tian E, Han Q-L. A delay system method for designing event-triggered controllers of networked control systems. IEEE Trans Autom Control 2013;58(2):475–81. https://doi.org/10.1109/TAC.2012.2206694

[30] Yoo J, Johansson KH. Event-triggered model predictive control with a statistical learning. IEEE Trans Syst Man Cybern Syst 2021;51(4):2571–81. https://doi.org/10.1109/TSMC.2019.2916626

[31] Ahmad I, Ge X, Han Q-L. Decentralized dynamic event-triggered communication and active suspension control of in-wheel motor driven electric vehicles with dynamic damping. IEEE/CAA J Autom Sin 2021;8(5):971–86. https://doi.org/10.1109/JAS.2021.1003967

[32] Wang J, Krstic M. Event-triggered adaptive control of coupled hyperbolic PDEs with piecewise-constant inputs and identification. IEEE Trans Autom Control 2023;68(3):1568–83. https://doi.org/10.1109/TAC.2022.3159292

[33] Ahmed I, Rehan M, Iqbal N. A novel exponential approach for dynamic event-triggered leaderless consensus of nonlinear multi-agent systems over directed graphs. IEEE Trans Circuits Syst II Express Briefs 2022;69(3):1782–6. https://doi.org/10.1109/TCSII.2021.3120791

[34] Liu J, Wang W, Hu B, Liu J, Xie XP, Tian E. Fuzzy-boosted event-triggered tracking control of unknown nonlinear networked systems: A PSO-driven RL approach. IEEE Trans Autom Sci Eng; 2025;22:7736–47. https://doi.org/10.1109/TASE.2024.3468614

[35] Chen G, Dong J. Data-driven control for discrete-time nonlinear systems with dual-channel dynamic event-triggered mechanism. IEEE Trans Circuits Syst II Express Briefs 2023;70(12):4439–43. https://doi.org/10.1109/TCSII.2023.3285769

[36] Liu J, Qian Y, Zha L, Tian E, Xie X. Adaptive event-triggered control for networked interconnected systems with cyber-attacks. Nonlinear Anal Hybrid Syst 2023;50:101377. https://doi.org/https://doi.org/10.1016/j.nahs.2023.101377

[37] Shen Y, Wang Z, Dong H, Liu H, Liu X. Joint state and unknown input estimation for a class of artificial neural networks with sensor resolution: An encoding-decoding mechanism. IEEE Trans Neural Netw Learn Syst 2025;36(2):3671–81. https://doi.org/10.1109/TNNLS.2023.3348752

[38] Li J, Wang Z, Dong H, Yi X. Outlier-resistant observer-based control for a class of networked systems under encoding-decoding mechanism. IEEE Syst J 2022;16(1):922–32. https://doi.org/10.1109/JSYST.2020.3044238

[39] Zou L, Wang Z, Shen B, Dong H. Encryption-decryption-based state estimation with multirate measurements against eavesdroppers: A recursive minimum-variance approach. IEEE Trans Autom Control 2023;68(12):8111–18. https://doi.org/10.1109/TAC.2023.3288624

[40] Zou L, Wang Z, Shen B, Dong H. Secure recursive state estimation of networked systems against eavesdropping: A partial-encryption-decryption method. IEEE Trans Autom Control 2024;:1–14. https://doi.org/10.1109/TAC.2024.3512413

[41] Wang L, Wang Z, Liu S, Peng D. Unscented Kalman filtering over full-duplex relay networks under binary encoding schemes. IEEE Trans Autom Control 2024;:1–8. https://doi.org/10.1109/TAC.2024.3521281

[42] Gao C, Wang Z, Hu J, Liu Y, He X. Consensus-based distributed state estimation over sensor networks with encoding-decoding scheme: Accommodating bandwidth constraints. IEEE Trans Netw Sci Eng 2022;9(6):4051–64. https://doi.org/10.1109/TNSE.2022.3195283

[43] Alalwan A, Mohamed T, Chakir M, Laleg TM. Extended Kalman filter based linear quadratic regulator control for optical wireless communication alignment. IEEE Photonics J 2020;12(6):1–12. https://doi.org/10.1109/JPHOT.2020.3037223

[44] Tao J, Wei C, Wu J, Wang X, Shi P. Nonfragile observer-based control for markovian jump systems subject to asynchronous modes. IEEE Trans Syst Man Cybern Syst 2021;51(6):3533–40. https://doi.org/10.1109/TSMC.2019.2930681

[45] Li X, Zhang T, Wu J. Input-to-state stability of impulsive systems via event-triggered impulsive control. IEEE Trans Cybern 2022;52(7):7187–95. https://doi.org/10.1109/TCYB.2020.3044003

[46] Tan Y, Yuan Y, Xie X, Tian E, Liu J. Observer-based event-triggered control for interval type-2 fuzzy networked system with network attacks. IEEE Trans Fuzzy Syst 2023;31(8):2788–98. https://doi.org/10.1109/TFUZZ.2023.3237846
[47] Zhang M, Shen C, Wu Z-G. Asynchronous observer-based control for exponential stabilization of markov jump systems. IEEE Trans Circuits Syst II Express Briefs 2020;67(10):2039–43. https://doi.org/10.1109/TCSII.2019.2946320